PROCEEDINGS OF SCIENCE

The Design and Status of the HELIX Ring Imaging Cherenkov Detector and Hodoscope Systems

H. B. Jeon,[a] **P. S. Allison,**[b] **M. Baiocchi,**[c] **J. J. Beatty,**[b] **L. Beaufore,**[a] **D. H. Calderón,**[b] **A. G. Castano,**[a] **Y. Chen,**[d] **S. Coutu,**[d] **N. Green,**[e] **D. Hanna,**[f] **S. B. Klein,**[g] **B. Kunkler,**[g] **M. Lang,**[g] **R. Mbarek,**[a] **K. McBride,**[b] **S. I. Mognet,**[d] **J. Musser,**[g] **S. Nutter,**[h] **S. O'Brien,**[f] **N. Park,**[c] **K. M. Powledge,**[a] **K. Sakai,**[a] **M. Tabata,**[i] **G. Tarlé,**[e] **J. M. Tuttle,**[a] **G. Visser,**[g] **S. P. Wakely**[a] **and M. Yu**[d]

[a] *University of Chicago, Dept. of Physics, Chicago, USA*
[b] *The Ohio State University, Dept. of Physics, Columbus, USA*
[c] *Queen's University, Dept. of Physics, Engineering Physics and Astronomy, Kingston, Canada*
[d] *Pennsylvania State University, Dept. of Physics, University Park, USA*
[e] *University of Michigan, Dept. of Physics, Ann Arbor, USA*
[f] *McGill University, Dept. of Physics, Montreal, Canada*
[g] *Indiana University, Dept. of Physics, Bloomington, USA*
[h] *Northern Kentucky University, Dept. of Physics, Geology and Engineering Technology, Highland Heights, USA*
[i] *Chiba University, Dept. of Physics, Chiba, Japan*

E-mail: hyebin@uchicago.edu

HELIX (High Energy Light Isotope eXperiment) is a balloon-borne experiment designed to measure the chemical and isotopic abundances of light cosmic-ray nuclei. Detailed measurements by HELIX, especially of ^{10}Be from ~0.2 GeV/n to beyond 3 GeV/n, will provide essential insights into the propagation processes of the cosmic rays. HELIX features a Ring Imaging Cherenkov (RICH) detector designed to measure the velocity and charge of nuclei with energies greater than ~1 GeV/n. The RICH detector consists of a radiator volume of high-transparency high-index aerogel tiles imaged by a ~1 m^2 focal plane instrumented by 200 8×8 arrays of silicon photomultipliers (SiPMs). A scintillating fiber hodoscope read out with SiPM arrays is installed on the top of the RICH radiator plane to improve the accuracy of track reconstruction in the non-bending view of the instrument's magnet spectrometer system. We present the design and current status of the HELIX RICH and hodoscope systems.

38th International Cosmic Ray Conference (ICRC2023)
26 July - 3 August, 2023
Nagoya, Japan

PoS(ICRC2023)121

1. Introduction

HELIX [1] is a balloon-borne experiment to measure the chemical and isotopic abundances of light cosmic-ray nuclei from protons to neon (Z=1-10), especially the ^{10}Be/^{9}Be ratio from ~0.2 GeV/n to beyond 3 GeV/n. Be is formed by spallation of heavier cosmic rays in the interstellar medium and decays with a half life of 1.4 Myr which is comparable to the containment time within the Galaxy. Therefore, measurements of the ^{10}Be/^{9}Be ratio can provide important data for understanding the propagation of cosmic rays.

The HELIX instrument is shown in Figure 1. The drift chamber tracker (DCT) under a 1 T magnetic field formed by superconducting magnet coils measures the rigidity of incident particles. For particles with energies less than ~1 GeV/n, the top and bottom time-of-flight detectors (TOF), with a separation of ~2.3 m, provide velocity measurements and charge measurements at all energies. Velocities of particles with energies exceeding this are obtained by the ring-imaging Cherenkov detector (RICH). A hodoscope located on top of the RICH is employed to reduce the uncertainty in trajectories of particles incident on the RICH in the non-bending view of the magnet. This contribution describes the RICH and hodoscope subsystems and presents their current status and plans. For more details on the HELIX experiment in general [2] and the DCT [3], see these other contributions at this conference.

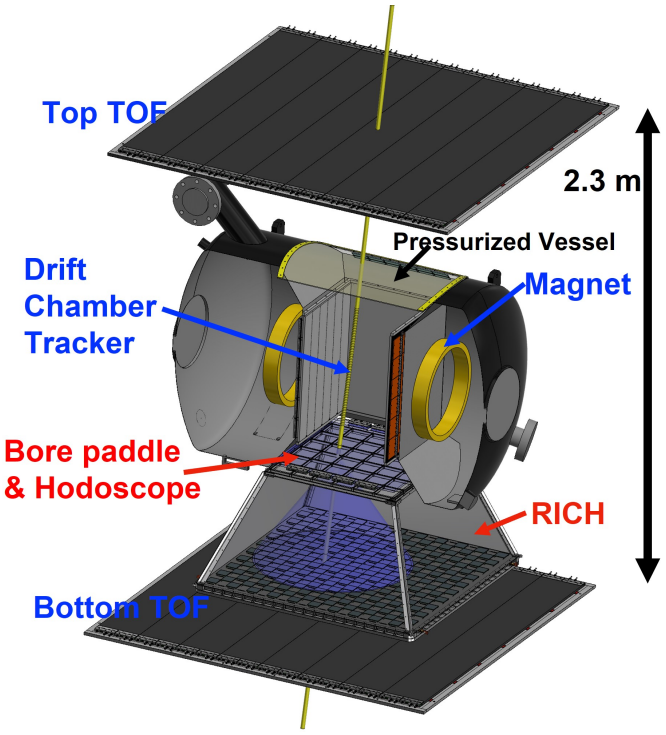

Figure 1: 3D model of the HELIX instrument in a partially-sectioned view with a particle with an energy of ~3 GeV/n going through.

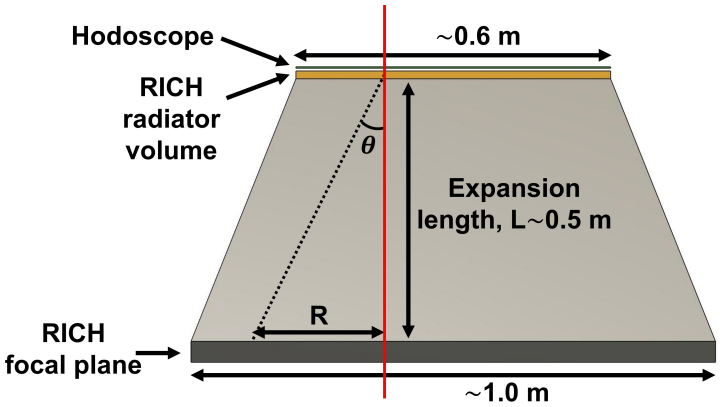

Figure 2: A drawing of the RICH and hodoscope in side view. The red line indicates a particle vertically passing through the RICH. The dashed line shows a cone shape of Cherenkov light with an emission angle of θ produced in the radiator and shining on the focal plane with a radius of R.

2. HELIX Ring-Imaging Cherenkov Detector

The HELIX RICH is a proximity-focused RICH designed to measure the velocity of particles radiating Cherenkov light in a medium by reconstructing rings of photons detected on a focal plane. From the impact parameter of the photon hits from the particle trajectory, the Cherenkov angle can be determined, leading to the particle velocity through the well-known formula

$$\beta = \frac{1}{n \cos\theta}, \tag{1}$$

where β is the particle velocity, n is the refractive index of the medium and θ is the emission angle. To achieve a Lorentz-weighted velocity resolution ($\gamma^2 d\beta/\beta$) of less than 2% up to particle energies of 3 GeV/n, the refractive index of the radiator must be known to an accuracy on the order of 10^{-4}. It is also essential to know accurately the expansion length between the focal plane and the radiators as well as the precise positions of the SiPMs on the focal plane.

The RICH consists of a radiator volume and focal plane with an expansion length of ~50 cm, as shown in Figure 2. In the radiator volume, which has an area of 60×60 cm^2, two different types of radiator tiles, both with dimensions of $10 \times 10 \times 1$ cm^3, are employed in a 6×6 array. The majority are 32 hydrophobic aerogel tiles, with four NaF tiles located at the corners. The focal plane, with an area of ~1 m^2, comprises custom Hamamatsu silicon photomultiplier (SiPM) arrays populated in a checkerboard pattern, shown in the left panel of Figure 3. Each array contains 64 individual SiPMs of size 6×6 mm^2, with 6336 micropixels on a 75um pitch.

The aerogel tile radiators are made with a novel pin-hole drying process to have high transparency and high refractive index of ~1.15 [4, 5]. A resolution of order 10^{-4} in refractive index has been achieved for the aerogel tiles. The details of the measurements are described in [6–8].

The SiPM arrays are read out by RICH front-end electronics boards through flexible PCB cables with a length of 70 cm, pictured in Figure 3. Each RICH front-end board contains 16 CITIROC 1A ASICs [9] with 32 channels allowing 8 SiPM arrays to be processed per board. Each CITIROC amplifies its signal and feeds it into two paths of fast and slow shapers generating a time

Figure 3: Left: A photo of the top view of the RICH. 200 SiPM arrays are populated on the focal plane in a checkerboard pattern. Right: A photo of the enclosed RICH detector. Flexible cables run from SiPM arrays on the focal plane. The locations of the cooling rail and Peltier module are indicated.

stamp with a resolution better than 12.5 ns and multiplexed charge output, respectively. On the timing path, an individual discriminator for each channel is used to suppress dark current noise, while the charge signal is a pulse height measured by a sample-and-hold circuit. The CITIROC can also adjust trim bias voltages for individual channels to equalize the gains of all the SiPMs. Due to the trim voltage linearity, a bias on a single SiPM, provided by CITIROC ASIC and the RICH front-end board, is determined by the sum of the common bias for all channels of the SiPM array and the corresponding trim voltage.

To control the temperature of the SiPMs, a liquid cooling system is employed, consisting of thermoelectric devices, a pump, a radiator and a reservoir. Lower temperatures are desired to suppress dark currents that are produced by thermal excitation in the sensors giving rise to random hit noise. To uniformly cool down all SiPMs, two Peltier thermoelectric modules (CP2-127-10-L1-W4.5, Laird Thermal Systems) are placed near two diagonal corners of the focal plane. The colder sides of the Peltier modules are thermally connected to ~65 cm-long cooling rails with heat pipes installed along two opposite sides of the focal plane. On the hotter side of each Peltier module, a heat exchanger is attached, with coolant to transfer the heat. The coolant, HC-50 from Dynalene Inc, absorbs heats from the RICH by circulating through the two heat exchangers in a row and then runs into a ~1 L reservoir. The liquid is pumped by a commercial pump (GJ-N21-DEMSE, Micropump) to a planar radiator with a dimension of 30×30 cm^2 to radiate to space. The chilled coolant then returns to the RICH. The cooling system is optimized for a flow rate of 380 mL/min to dissipate the heat from the RICH out of the instrument.

To obtain precise measurements of the expansion length, L, and positions of the SiPMs on the focal plane, a Handyscan 307 (CREAFORM) device is used which can produce a 3D model of a scanned object with a 0.025 mm accuracy [10]. Once the focal plane and radiator volume are assembled together but before the placement of sensors and radiators, they are 3D-scanned to determine an accurate expansion L which is crucial for calculating the angle term in Eq.1. The SiPM arrays are then populated to form the focal plane and 3D scanning is carried out again to

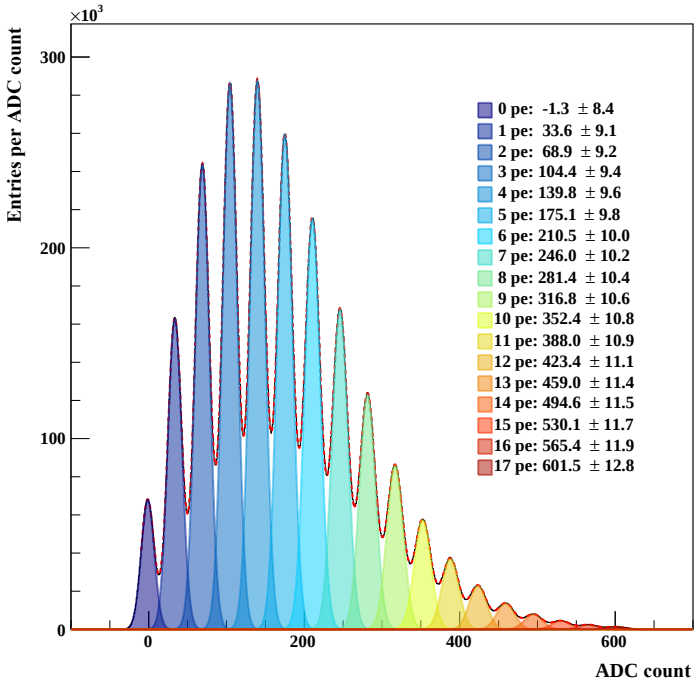

Figure 4: A superposition of photoelectron (PE) signals of the 12,697 gain-matched SiPM channels of the RICH focal plane with multiple Gaussian fits. The noisy channels, 0.8% out of all SiPMs, are excluded in this analysis due to being noisy, dead or controlled by a problematic CITIROC. Clear peak separation with a spacing of ~36 ADC counts is shown up to 17 PEs sensed by SiPM arrays illuminated by a pulsed laser. The legend displays the corresponding number of PEs and mean±sigma of the Gaussian fitting.

obtain the exact position of the sensors on the focal plane. The length, including L and the radiator thickness, is found to be 516.6 ± 0.7 mm from the 3D scan measurements. The measured SiPM 2D positions are consistent with the nominal locations with a residual of -0.1 ± 0.2 mm. The focal plane formed by the top surfaces of the SiPMs is uniform to 0.1 mm.

Gain matching of the SiPMs ensures that every SiPM produces the same amount of charge in response to a single photoelectron (PE). The desired SiPM gains are determined by adjusting the common bias and trim voltages. For this purpose, the focal plane is illuminated using a nanosecond pulsed laser diode system (NPL41B, THORLABS) and a fiber cannula diffuser tip (CFDSB05, THORLABS) at the end of the optical fiber. The laser pulse is synchronized using a pulse generator with an external trigger fed to the HELIX data acquisition (DAQ) system. As laser pulses are accumulated, bias voltages are scanned to determine a common voltage that would satisfy all channels in the SiPM array if a trim voltage within the linear range were applied. At the selected common bias, the trim voltage is then scanned in order to fine-tune the bias for individual channels.

All 200 SiPM arrays are gain-matched using these scan data. Figure 4 depicts the superposition of the charge distributions of the SiPMs fitted with multiple Gaussian functions implying number of PEs by spacing from the peak of 0 PE distribution. 0.8% of the SiPMs are excluded because they are noisy, dead or controlled by a problematic CITIROC. The legend in the figure displays the

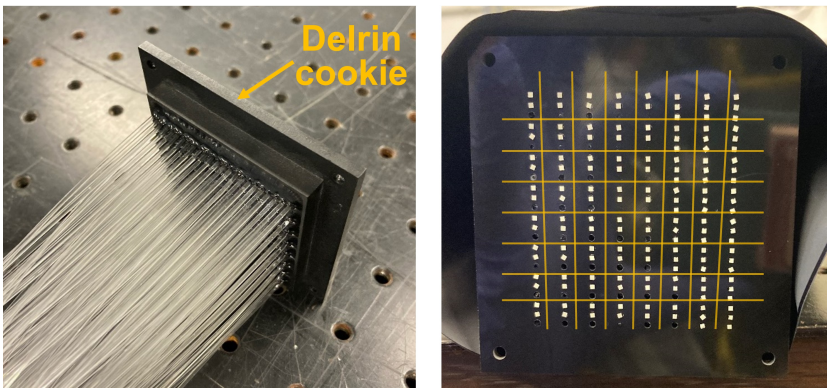

Figure 5: Left: A photo of a Delrin cookie in which a fiber ribbon terminates. Right: A photo of the back side of the Delrin cookie with a multiplexing pattern. The yellow grid lines indicate SiPM pixel channel separations.

corresponding number of PEs and mean and sigma of the fitting. 99.2% of 12,800 SiPM channels on the focal plane shows remarkable agreement with clear peak separations with a uniform spacing of ~36 ADC, for this gain setting.

3. HELIX Hodoscope

A scintillating fiber hodoscope has been introduced directly above the radiators in order to improve the RICH performance by reducing uncertainties in the trajectories of particles entering the radiators. The hodoscope consists of four 150-fiber ribbons arranged in a single layer. Each ribbon is made of BCF12 plastic scintillating fibers from Saint-Gobain Crystals; each fiber has a 1 mm × 1mm square cross section and a length of 1 m. The active hodoscope area is 60 cm × 60 cm covering the full radiator volume. The end of a fiber bundle of the ribbon is terminated in a Delrin cookie with a position-multiplexed pattern wherein two or three fibers with a separation of ~64 mm are assigned to a single SiPM in an 8×8 array which is the same sensor used for the RICH. The outputs of the SiPM arrays are read out by the RICH front-end board.

The ribbons are individually wrapped in light-tighting Tedlar sheets. Because the flexible fiber ribbons are not completely colinear, a table must be generated to map 2D fiber positions to channel IDs. This is done by scanning the active area with a collimated ^{90}Sr radioactive source. The mapping was performed by placing the source stepwise over a grid of points covering the active area. Step sizes were 1 mm in the X direction and 50 mm in the Y direction, where X and Y axes are the non-bending and bending axes of the magnet. Using a known source position, the irradiated fiber was found by fitting a distribution of signal rates as a function of fiber IDs. A map of the 600 fibers has been achieved from a total of ~9,000 measurements. Figure 6a shows an example of the reconstructed fibers in the XY plane of the hodoscope.

In addition, a 0.33 mm spatial resolution of the hodoscope is achieved (preliminary) including the uncertainties from intrinsic fiber dimension, the measurement system, the mapping process, and systematic effects. This result implies the hodoscope can improve uncertainties of particle trajectories at the radiators in the non-bending view by a factor of more than 10 compared to using only the drift-chamber measurements.

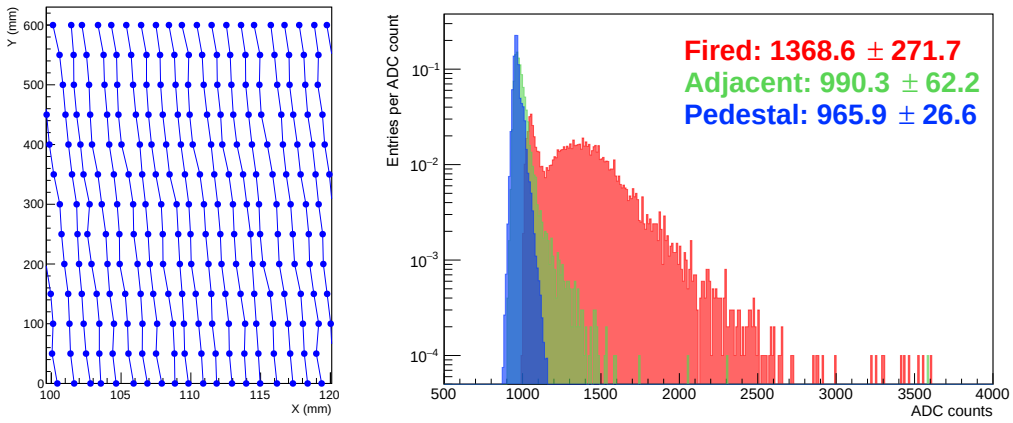

(a) **(b)**

Figure 6: (a) A part of the reconstructed positions of the 600 fibers in the XY plane of the active area of the hodoscope, where the X and Y axes are along the non-bending and bending directions of the magnet, respectively. (b) Charge signal distributions of cosmic-ray muons from the stand-alone hodoscope test. “Fired” in red indicates a fiber with the largest signal in an event, and “adjacent” in green shows the average of the signals from the two fibers on either side of the fired one. The "pedestal" distribution of all SiPMs in an array is shown in blue. The legend displays the mean and standard deviation of each distribution.

In a separate test, the hodoscope was tested with cosmic-ray muons using a small scintillator telescope and the HELIX readout infrastructure. Figure 6b presents charge distributions of "fired", "adjacent" and "pedestal" signals. “Fired” means a signal from a fiber with the largest signal in an event, which is regarded as a channel with a muon hit. “Adjacent” is the average of the signals from the two fibers on either side of the fired one. The pedestal distribution is taken with a random trigger. The signal ratio between the adjacent and fired fibers is (preliminary) ~8%, which may be explained by corner-clipping tracks, as well as crosstalk in the fiber and electronics.

4. Current status and plans

The RICH and hodoscope have been fully assembled and tested. The RICH has been inspected by 3D scanning to determine a precise expansion length and positions of the SiPM arrays on the focal plane. The uniform gains of the 200 SiPM arrays, 12,800 channels in total, across the focal plane has been achieved by adjusting bias voltages for the individual channels. For the hodoscope, as the fibers are not perfectly colinear to each other, more than 9,000 measurements with a radioactive source across the active area have been performed to obtain a map of fiber locations. From the measurements, a preliminary spatial resolution of 0.33 mm has been achieved. The hodoscope with the HELIX readout system has been verified to detect ground-level cosmic-ray muons.

A first HELIX long-duration balloon flight is scheduled for late spring 2024 from Kiruna, Sweden to northern Canada.

Acknowledgements

This work is supported in the US by grant 80NSSC20K1840 from the National Aeronautics and Space Administration (NASA) and in Canada by grants from the Natural Sciences and Engineering Research Council (NSERC) and the Canadian Space Agency's Flights and Fieldwork for the Advancement of Science and Technology (FAST) program.

References

[1] N. Park *et al.*, in Proc. of the 37th International Cosmic Ray Conference (Berlin) , 091 (2021).

[2] N. Park *et al.*, in Proc. of the 38th International Cosmic Ray Conference (Nagoya) , CRD6 (2023).

[3] McBride *et al.*, in Proc. of the 38th International Cosmic Ray Conference (Nagoya) , PCRD0 (2023).

[4] M. Tabata *et al.*, Nuclear Instruments and Methods in Physics Research Section A **623**, 339 (2010), 1st International Conference on Technology and Instrumentation in Particle Physics (Tsukuba).

[5] P. Allison *et al.*, in Proc. of the 36th International Cosmic Ray Conference (Madison) , 139 (2019).

[6] O'Brien *et al.*, in Proc. of the 37th International Cosmic Ray Conference (Berlin) , 090 (2021).

[7] P. Allison *et al.*, in Proc. of the 36th International Cosmic Ray Conference (Madison) , 133 (2019).

[8] P. Allison *et al.*, Nuclear Instruments and Methods in Physics Research Section A (In Press) (2023).

[9] J. Fleury *et al.*, Journal of Instrumentation **9** (01), C01049.

[10] Creaform handyscan 307, https://www.creaform3d.com [Accessed: 2023/07/11].